

ÇAÍ OIL AS AN ALTERNATIVE IN THE SYNTHESIS AND COATING OF IRON OXIDE NANOPARTICLES

Suane C. Paes¹, Bruno S. Corrêa², Cleidilane Sena¹, Messias S. Costa¹, Gabriel A. Cabrera-Pasca¹, Artur W. Carbonari² and Mitiko Saiki²

¹ Faculdade de Ciências Exatas e Tecnologias (FACET / UFPA)
Universidade Federal do Pará
Rua Manuel de Abreu, s/n
68440-000 Abaetetuba, PA
suanecastro26@hotmail.com
cleidilane@ufpa.br
mscosta@ufpa.br
gpasca@gmail.com

² Instituto de Pesquisas Energéticas e Nucleares (IPEN / CNEN - SP)
Av. Professor Lineu Prestes 2242
05508-000 São Paulo, SP, Brazil
bruno27ni@gmail.com
carbonar@ipen.br
mitiko@ipen.br

ABSTRACT

In the last decades, nanotechnology studies have attracted the attention of researchers from various fields, engineering, chemistry, physics, medicine, environment. Medicine, nanomedicine, the major advances in the diagnosis and therapies of diseases, such as magnetic resonance imaging and the treatment of cancer by hyperthermia, respectively. Nanomaterials for such biomedical applications should have size control of less than 20 nm, crystal structure and well-defined morphology. Thus, as nanoparticles of iron oxide (Fe_3O_4) is one of the materials most studied for such applications. Thus, iron oxide nanoparticles were synthesized by variation of the thermal decomposition method, which is described as one of the best quality nanoparticle synthesis tools. During the synthesis, we used açai oil, rich in fatty acids, palmitoleic, linoleic and palmitic, as a process of synthesis and coating of nanoparticles, making them biocompatible. The açai oil was made by the supercritical extraction method, where the product can be obtained pure, free of solvents. The samples were characterized by X-ray diffraction (XRD) and the magnetite phase (Fe_3O_4) was identify through the position of the intensity peaks. The nanoparticles present spherical morphology with a diameter of 3 to 10 nm, observed through transmission electron microscopy (TEM) images. In addition, neutron analysis (NAA) determined that the samples had a concentration of 74.93% Fe_3O_4 and a remaining database is related to the coating of sample nanoparticles as potentiated for biomedical applications.

1. INTRODUCTION

In the last decades, magnetic materials at the nanometer scale, with dimensions ranging from 1 to 100 nm have received great attention from researchers from different areas (chemistry, physics, engineering and medicine) who are studying their properties in a wide variety of biomedical applications such as controlled drug delivery, magnetic resonance imaging contrast agent, immobilization and separation of biomolecules, hyperthermia. However, the

major advances are focused on the diagnosis of diseases by magnetic resonance imaging and the treatment of cancer by hyperthermia [1-6].

Magnetic nanoparticles for biomedical applications need to be mainly biocompatible and non-toxic, to have size and shape control, high crystallinity, reproducibility and good dispersion on substrates and solutions, generating a great demand for high quality materials [4,5].

Thermal decomposition is one of the best methods of quality nanoparticle synthesis [7-9]. Thus, nanoparticle samples of iron oxide (Fe_3O_4) were synthesized by modifying the thermal decomposition method using açai oil (*Euterpe oleracea*), as an alternative in the process of synthesis and coating of nanoparticles, making them biocompatible and not toxic. Vegetable oils are mostly non-toxic and biocompatible, and their use as a solvent and stabilizing agent in the synthesis of nanoparticles is based on the concept of green chemistry and biocompatibility [10].

The oil of the pulp of the fruit of the açai tree extracted by the method of extraction with supercritical fluid is free of solvents, pure, and rich in fatty acids in different proportions, being that in greater concentration they are the oleic, palmitoleico, linoleico and palmitic acids [11].

The magnetite (Fe_3O_4) has a cubic structure and space group $\text{Fd}\bar{3}\text{m}$, with a network parameter of 8.394 Angstrom, and is composed of Fe^{2+} ions and half of the Fe^{3+} ions distributed in the octahedral sites (O site) and the other half of the Fe^{3+} ions occupying the sites tetrahedral (site T). It is a promising candidate among magnetic nanomaterials for biomedical applications [12-14].

The synthesized samples were characterized by the X-ray diffraction (XRD) technique, to verify the formation of Fe_3O_4 nanoparticles; transmission electron microscopy (TEM), to observe the morphology and grain size distribution; neutron activation analyzes (NAA), to determine the concentration of Fe_3O_4 present in the samples.

2. MATERIALS AND METHODS

2.1. Supercritical CO_2 extraction

Açai oil (*Euterpe oleracea*) was obtained by the supercritical CO_2 extraction method using a SPE-ED SFE Applied Separations extraction equipment, model 7071 (Allentown, PA, USA). The volume of the extraction cell was $5 \times 10^{-5} \text{ cm}^3$. The extraction was carried out at a pressure of 320 bar, temperature of 70 °C and density of $800 \text{ kg}\cdot\text{m}^{-3}$, using CO_2 (99.9% purity) with a flow rate of $8.85 \times 10^{-5} \text{ kg}\cdot\text{s}^{-1}$, as described in the work published by Batista et al [11].

2.2. Synthesis of iron oxide nanoparticles

The samples of iron oxide nanoparticles were synthesized by modification of the thermal decomposition method described by Oliveira et al [8] which consisted in the dissolution of 2 mmol of iron (III) acetylacetonate in 20 mL of a high boiling solvent (diphenyl ether)

together with 2 mL of açaf oil, 4 mmol of oleylamine and 10 mL of 1,2-octanediol. The mixture was heated and allowed to stir under nitrogen at reflux for three hours. After cooling to room temperature, the nanoparticles were purified 3 times by centrifugation (5000 rpm) in ethanol for 30 minutes. The nanoparticles are then powdered after drying under vacuum.

2.3. X-Ray Diffraction

To verify the formation of the Fe₃O₄ nanoparticles, X-ray diffraction (XRD) measurements of the powder sample were performed using a PANalytical X-ray diffractometer, X'Pert PRO model with X'Celerator detector, using Cu K α radiation ($\lambda_{\alpha 1} = 0.154060$ nm and $\lambda_{\alpha 2} = 0.154443$ nm) and operating at 40 kV voltage and 40 mA current. Data collection was performed at a step size of 0.05 °.

Through the XRD incident on the material it is possible to reconstruct the periodic structure of the material using the Bragg law, given by Equation 1.

$$n\lambda = 2dsen\theta \quad (1)$$

in which, n is the order of diffraction, λ is the wavelength and θ is the angle between the incident X-rays and the atomic planes [15].

2.4. Transmission electronic microscopy

To observe the morphology and size distribution of the iron oxide nanoparticles, transmission electron microscopy (TEM) measurements were performed using a JEOL JEM 2100, operating with a 200 kV acceleration voltage. A drop of solution containing Fe₃O₄ nanoparticles dispersed in toluene was deposited on a copper grid for observation and micrographs of the nanoparticles.

2.5. Neutron Activation Analysis

Neutron activation analysis (NAA) was performed to determine the concentration of Fe₃O₄ present in the samples. A mass of 30.58 mg of the powder sample was irradiated, along with a synthetic Fe standard, in the IEA-R1 nuclear reactor. The irradiation time was 16 h under a thermal neutron flux of 5.4×10^{12} n.cm⁻² s⁻¹. After one week of decay, the gamma activities of the irradiated sample and the Fe standard were measured using a hyperpure Ge detector connected to a DSA 1000 Digital Spectrum Analyzer, both of the Canberra brand. The Fe element was identified by the measurement of ⁵⁹Fe by the energies of gamma rays of 1099.25 and 1291.60 keV and half life of 44.5 d. The Fe concentration was calculated by the comparative method described by De Soete et al [16] by means of the following relation, Equation 2.

$$C_a = \frac{m_p.A_a.e^{\left[\frac{0,693.(tda-tdp)}{t_{1/2}}\right]}}{M_a.A_p} \quad (2)$$

the indices a and p samples are a sample and the standard, M_a is total sample mass, m_p is mass of the standard, C_a is Fe concentration in the sample, A is radioisotope activity after a

certain time of decay, $t_{1/2}$ is life time of the radioisotope considered and td is the decay time.

3. RESULTS AND DISCUSSIONS

The X-ray diffraction spectrum as a function of 2θ of the nanoparticle samples synthesized with açai oil shows the position of the peaks associated with their respective crystallographic planes, as shown in Fig. 1, are in accordance with the results shown in [8,9,13,17], indicating that the synthesized material corresponds to Fe_3O_4 nanoparticles, spatial group $\text{Fd}3\text{m}$.

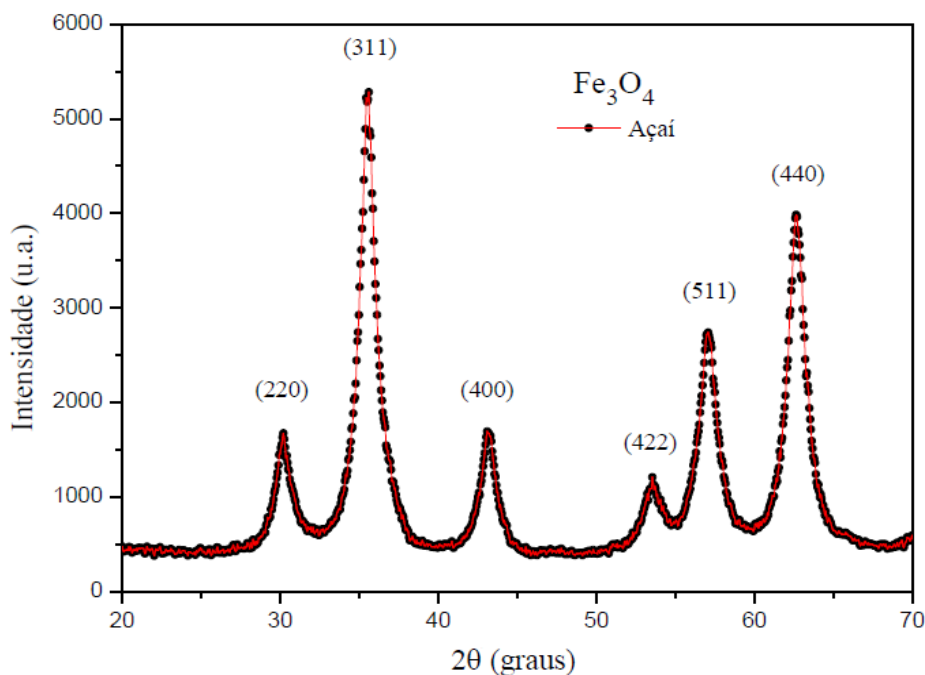


Figure 1: X-ray diffraction spectrum of the Fe_3O_4 nanoparticle samples synthesized with açai oil.

TEM images indicate that the iron oxide particles synthesized with açai oil have spherical morphology, with mean diameter and standard deviation of 4.09 nm and 1.08 nm, respectively, as shown in Fig 2. These results are satisfactory, since in their published works Oliveira et al [8] and Effenberger et al [9] synthesized, by the thermal decomposition method and with totally synthetic reagents, Fe_3O_4 nanoparticles with a diameter of 8 nm and 5.6 nm, respectively, whereas, Matos et al [13] synthesized nanoparticles of iron oxide by co-precipitation with mean diameters of 12 nm. With respect to the NAA results, it was verified that 74.93% of the nanoparticles are formed by Fe_3O_4 and the remaining mass percentage, 25.07%, consists of carbon chain materials, probably of the fatty acids present in açai oil, which may be coating the nanoparticles.

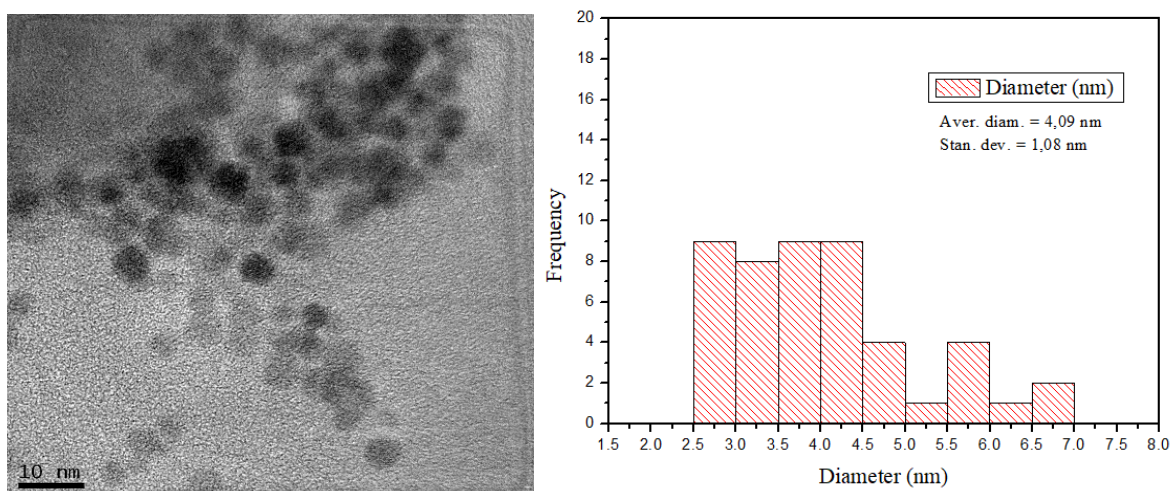


Figure 1: Transmission electron microscopy images of iron oxide nanoparticles synthesized with açai oil.

However, the use of açai oil as an alternative in the synthesis of Fe_3O_4 nanoparticles by the thermal decomposition method is satisfactory, since the results are in agreement with the literature [8,9,13,17].

4. CONCLUSIONS

Nanoparticles of Fe_3O_4 were synthesized by the thermal decomposition method using açai oil. Results of XRD and TEM indicate the formation of a single phase of magnetite (Fe_3O_4), with the formation of spherical nanoparticles, with narrow distribution and size control (4.09 nm). And NAA results show that the nanoparticles are mostly (74.93%), made up of Fe_3O_4 that may be coated with (25.07%) carbon chain materials that constitute the fatty acids present in the açai oil. Therefore, these results may contribute to future biomedical applications. However, characterizations of the magnetic and electrical properties must be performed.

REFERENCES

1. Y. Cheng, L. Yin, S. Lin, M. Wiesner, E. Bernhardt, J. Liu, "Toxicity Reduction of Polymer-Stabilized Silver Nanoparticles by Sunlight," *J. Phys. Chem.*, **115**, pp.4425-4432 (2011).
2. R. Lehner, X. Wang, S. Marsch, P. Hunziker, "Intelligent nanomaterials for medicine: Carrier platforms and targeting strategies in the context of clinical application," *Nanomedicine: Nanotechnology, Biology, and Medicine*, **9**, pp.742-757 (2013).
3. S. Nazir, T. Hussain, A. Ayub, U. Rashid, A. J. MacRobert, "Nanomaterials in combating cancer: Therapeutic applications and developments," *Nanomedicine: Nanotechnology, Biology, and Medicine*, **10**, pp.19-34 (2014).
4. A. Ito, M. Shinkai, H. Honda, T. Kobayashi, "Medical Application of Functionalized Magnetic Nanoparticles," *J. Biosci. Bioeng.*, **100**, pp.1-11 (2005).

5. L. Zhou, J. Yuan, Y. Wei, "Core-shell structural iron oxide hybrid nanoparticles: from controlled synthesis to biomedical applications," *J. Mater. Chem.*, **21**, pp.2823-2840 (2011).
6. X. Ren, H. Chen, V. Yang, D. Sun, "Iron oxide nanoparticle-based theranostics for cancer imaging and therapy," *Front. Chem. Sci. Eng.*, **8(3)**, pp. 253-264 (2014).
7. S. H. Sun, H. Zeng, "Size-controlled synthesis of magnetite nanoparticles," *J. Am. Chem. Soc.*, **124**, pp.8204-8205 (2002).
8. F. C. C. Oliveira, F. B. Effenberger, M. H. Sousa, R. F. Jardim, P. K. Kiyohara, J. Dupont, J. C. Rubim, L. M. Rossi, "Ionic liquids as recycling solvents for the synthesis of magnetic nanoparticles," *Phys. Chem. Chem. Phys.*, **13**, pp.13558-13564 (2011).
9. F. B. Effenberger, A. W. Carbonari, L. M. Rossi, "The influence of 1,2-alkanediol on the crystallinity of magnetite nanoparticles," *J. Magn. Magn. Mater.*, **417**, pp.49-55 (2016).
10. S. F. A. Morais, M. G. A. Da Silva, E. C. Da Silva, A. M. F. De Melo, L. H. Pacheco, M. R. Meneghetti, "Síntese e estabilização de nanopartículas de ouro em óleo de mamona," *Rev. Virtual Quim.*, **5**, pp.95-105 (2013).
11. C. C. R. Batista, M. S. Oliveira, M. E. Araújo, A. M. C. Rodrigues, J. R. S. Botelho, A. P. S. Souza Filho, N. T. Machado, R. N. Carvalho Junior, "Supercritical CO₂ extraction of açai (Euterpe oleracea) berry oil: global yield, fatty acids, allelopathic activities, and determination of phenolic and anthocyanins total compounds in the residual pulp," *J. of Supercritical Fluids*, **107**, pp.364-369 (2016).
12. M. E. Fleet, "The structure of magnetite," *Acta Cryst.*, **37**, pp.917-920 (1981).
13. I. T. Matos, B. Bosch-Santos, G. A. Cabrera-Pasca, A. W. Carbonari, "Magnetic behavior of La-doped Fe₃O₄ studied by perturbed angular correlation spectroscopy with ¹¹¹Cd and ¹⁴⁰Ce," *J. Appl. Phys.*, **117**, pp.511-514 (2015).
14. J. Noh, O. I. Osman, S. G. Aziz, P. Winget, J. L. Jean-Luc Brédas, "Magnetite Fe₃O₄ (111) Surfaces: Impact of defects on structure, stability, and electronic properties," *Chem. Mater.*, **27**, pp.5856-5867 (2015).
15. W. D. Callister Jr, *Fundamentos da ciência e engenharia de materiais: uma abordagem integrada*. LTC, 2^a ed., Rio de Janeiro/Brazil (2006).
16. D. De Soete, R. Gijels, J. Hoste, *Neutron activation analysis*, Wiley-Interscience, London (1972).
17. M. R. Mauricio, H. R. Barros, M. R. Guilherme, G. M. Carvalho, "Synthesis of highly hydrophilic magnetic nanoparticles of Fe₃O₄ for potential use in biologic systems," *Colloids and Surfaces A: Physicochem. Eng. Aspects*, **417**, pp.224-229 (2013).